BIOCHEMISTRY
including biophysical chemistry & molecular biology

Article

pubs.acs.org/biochemistry

Examining Docking Interactions on ERK2 with Modular Peptide Substrates

Sunbae Lee,[†,^] Mangalika Warthaka,[†,^] Chunli Yan,[‡] Tamer S Kaoud,[†,§] Pengyu Ren,[*,‡,∥,⊥] and Kevin N. Dalby[*,†,§,∥,⊥,#]

[†]Division of Medicinal Chemistry and [‡]Department of Biomedical Engineering and Graduate Programs in [§]Pharmacy, [∥]Cell and Molecular Biology, [⊥]Biomedical Engineering, and [#]Biochemistry, University of Texas at Austin, Texas 78712, United States

ABSTRACT: ERK2 primarily recognizes substrates through two recruitment sites, which lie outside the active site cleft of the kinase. These recruitment sites bind modular-docking sequences called docking sites and are potentially attractive sites for the development of non-ATP competitive inhibitors. The D-recruitment site (DRS) and the F-recruitment site (FRS) bind D-sites and F-sites, respectively. For example, peptides that target the FRS have been proposed to inhibit all ERK2 activity (Galanis, A., Yang, S. H., and Sharrocks, A. D. (2001) *J. Biol. Chem. 276*, 965−973); however, it has not been established whether this inhibition is steric or allosteric in origin. To facilitate inhibitor design and to examine potential coupling of recruitment sites to other ligand recognition sites within ERK2, energetic coupling within ERK2 was investigated using two new modular peptide substrates for ERK2. Modeling shows that one peptide (Sub-D) recognizes the DRS, while the other peptide (Sub-F) binds the FRS. A steady-state kinetic analysis reveals little evidence of thermodynamic linkage between the peptide substrate and ATP. Both peptides are phosphorylated through a random-order sequential mechanism with a k_{cat}/K_m comparable to Ets-1, a bona fide ERK2 substrate. Occupancy of the FRS with a peptide containing a modular docking sequence has no effect on the intrinsic ability of ERK2 to phosphorylate Sub-D. Occupancy of the DRS with a peptide containing a modular docking sequence has a slight effect (1.3 ± 0.1-fold increase in k_{cat}) on the intrinsic ability of ERK2 to phosphorylate Sub-F. These data suggest that while docking interactions at the DRS and the FRS are energetically uncoupled, the DRS can exhibit weak communication to the active site. In addition, they suggest that peptides bound to the FRS inhibit the phosphorylation of protein substrates through a steric mechanism. The modeling and kinetic data suggest that the recruitment of ERK2 to cellular locations via its DRS may facilitate the formation of F-site selective ERK2 signaling complexes, while recruitment via the FRS will likely inhibit ERK2 through a steric mechanism of inhibition. Such recruitment may serve as an additional level of ERK2 regulation.

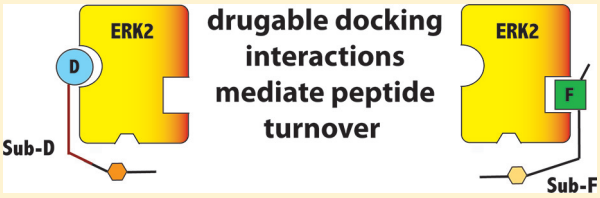

ERK2 plays an integral role in regulating biological processes in eukaryotic organisms.[1,2] They primarily recognize substrates through two recruitment sites, which lie outside the active site cleft of the kinase. These recruitment sites bind modular-docking sequences called docking sites[3] and are attracting interest as potential target sites for non-ATP competitive inhibitors (reviewed in ref 4). The D-recruitment site (DRS) and the F-recruitment site (FRS) bind D-sites and F-sites, respectively.[5−8] Figure 1 shows the general structural organization of ERK2 and the positions of the DRS and FRS on its surface relative to the active site cleft. While all the MAPKs are thought to possess a DRS, the FRS appears to be a feature common only to ERK1/2 and p38 MAPKα;[9−11] however, evaluations of ERK5 and other MAPKs such as ERK3 and ERK7 have not been reported.

A D-site contains a conserved $(R/K)_{2-3}-X_{2-6}-\Phi_A-X-\Phi_B$ sequence where Φ_A and Φ_B are hydrophobic residues. Crystal structures of MAP kinases in complex with D-site peptides [12] have shown that basic residues of a D-site can bind to a negatively charged surface on the MAPK termed Φ_{chg} in Figure 1, which contains two Asp residues previously identified as the common-docking domain.[13] However, recent NMR studies have suggested that not all D-sites engage the Asp residues of the Φ_{chg} site.[14] The $\Phi_A-X-\Phi_B$ sequence binds to a nearby hydrophobic pocket termed Φ_{hyd} in Figure 1. The two sites, Φ_{chg} and Φ_{hyd}, constitute the D-recruitment site (DRS).

The FRS binds a second docking motif termed an F-site, or the "DEF" motif (docking site for ERK FXFP), which was first characterized as an FXFP sequence.[15−17] This site is conserved in multiple ERK targets including Elk-1, c-Fos, SAP1, and the kinase suppressor of Ras (KSR).[6,15] More recently, a library-scan analysis suggested that either of the phenylalanines in the F-site motif may be substituted for tyrosine or tryptophan.[11] Unlike the DRS, no clear crystallographic information exists for the nature of the interactions that define the F-recruitment site (FRS). However, key residues that define this site have been identified using elegant hydrogen exchange mass spectrometry (HXMS) coupled with mutational analysis.[6] It was shown that Y231, L232, and L235 on one side of a hydrophobic groove on ERK2 together with M197, L198, and Y261 were crucial in defining the FRS and interacting with F-site sequences.

Received: July 16, 2011
Revised: September 24, 2011
Published: September 28, 2011

ACS Publications © 2011 American Chemical Society

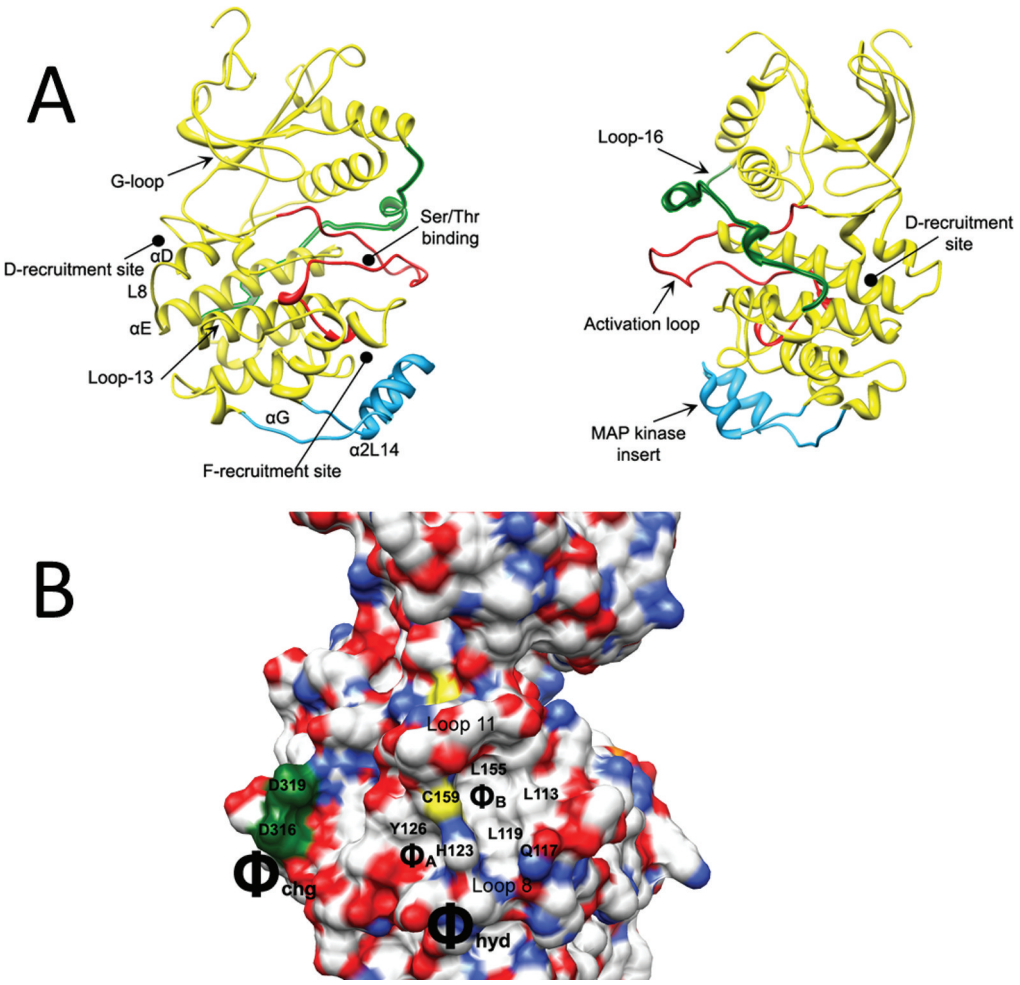

Figure 1. Diagrams of activated ERK2 (PDB 2ERK) showing the following. (A) The G-loop, which clamps onto ATP, and the binding site for substrate Ser/Thr-Pro motifs (which become phosphorylated). Also indicated are the D and F recruitment sites and loop-16 (green), which communicates between the D-recruitment site and the activation loop (red). A small insert, unique to MAP kinases, called the MAPK insert is also shown (*colored blue*, residues 246−276). The D-recruitment site comprises the common-docking domain and two hydrophobic areas (Φ_A and Φ_B) as shown in Figure 1B. The F-recruitment site (indicated) is a hydrophobic pocket with a preference for binding a ψ−X−ψ motif (where ψ are aromatic residues). (B) A negatively charged surface on the MAPK termed Φ_{chg}, which two Asp residues (D319 and D316) previously identified as the common-docking domain. A nearby hydrophobic site termed Φ_{hyd} (which consist with two hydrophobic areas Φ_A and Φ_B). The two sites, Φ_{chg} and Φ_{hyd}, constitute the D-recruitment site (DRS).

Mutation of the residues Y231, L232, L235, and Y261 to alanine in active ERK2 leads to significant reduction in binding.[6] These data allowed a model of an F-site peptide from Elk-1 bound at the FRS to be obtained.[6] (See also ref 18 for a related model.)

Substrates of ERK2 may be recognized through canonical modular docking interactions with the DRS, the FRS, or both[19] and in addition may also utilize more extensive noncanonical docking interactions. For example, we recently showed that while the *N*-terminus of the transcription factor Ets-1 binds to the Φ_{hyd} site of the DRS its SAM domain binds to the MAP kinase insert of ERK2.[18,20,21] Recent studies have evaluated the relative contributions of the FRS and the DRS in the recognition of a number of substrates.[18,19]

Using point mutations to impair binding at either the FRS or DRS of ERK2, Dimitri et al. showed that single canonical docking interactions are capable of supporting recognition and turnover of certain protein substrates,[22] suggesting that the docking interactions may function independently, a notion supported by the recent studies reported by Burkhard et al.[19] However, Glanis et al. have reported that F-site peptides inhibit all ERK2 activity.[9] The question of whether such inhibition is steric or allosteric in origin has not been resolved. Recently, our modeling studies suggested that an F-site peptide impedes the interaction between the SAM domain of Ets-1 and the MAPK insert of ERK2 through a steric mechanism.[18] However, hydrogen exchange mass spectrometry (HXMS) studies have revealed changes in ERK2 dynamics at significant distance from the FRS upon docking an F-site peptide, supporting a possible allosteric mechanism of inhibition.[6]

The purpose of this study was to evaluate the mechanism of inhibition of ERK2 by F-site peptides and to assess whether canonical docking interactions at one recruitment site communicate to distal sites to affect catalysis.[23] Peptide substrates of ERK2 that are recognized by the active site are phosphorylated with low efficiency;[24,25] however, peptides that utilize modular docking interactions exhibit significantly improved rates of phosphorylation.[26−28] Here we designed two new peptides that exclusively recognize either the DRS or the FRS and show that both peptides are phosphorylated with a

dx.doi.org/10.1021/bi201103b | *Biochemistry* 2011, 50, 9500−9510

specificity constant (k_{cat}/K_m) comparable to that of the protein substrate Ets-1.[29] We provide the first evaluation of the kinetic mechanism for such modular peptides. Our kinetic analysis suggests that while docking interactions are not communicated to each other, weak communication may occur from the DRS to the active site. Both peptides represent excellent tools with which to examine small molecule interactions at the recruitment sites. These studies suggest that F-site peptides probably inhibit ERK2 through a steric mechanism, suggesting that small molecules that locate to the FRS have potential to exhibit substrate selectivity.

EXPERIMENTAL PROCEDURES

Reagents. NovaSyn TGR resin was purchased from Novabiochem (Gibbstown, NJ). Fmoc-6-aminohexanoic acid was purchased from AnaSpec (Fremont, CA). Other Fmoc-amino acids, HBTU, and HOBT were obtained from Advanced ChemTech (Louisville, KY). Ultrapure grade Tris and HEPES were obtained from Sigma (St. Louis, MO). MP Biomedicals (Irvine, CA) supplied [γ-^{32}P]-ATP. P81 ion exchange cellulose chromatography paper was purchased from Whatman (Piscataway, NJ). Yeast extract, tryptone, agar, and IPTG were obtained from US Biologicals (Swampscott, MA). Ni-NTA agarose was supplied by Qiagen Inc. (Valencia, CA). A Mono Q HR 10/10 anion-exchange column was purchased from Amersham Biosciences (Piscataway, NJ). The *Escherichia coli* strain BL21 (DE3) used for recombinant protein expression was obtained from Invitrogen. The remaining molecular biology reagents, including protein molecular mass standards, were obtained from Invitrogen Corp. All other buffer components and chemicals were obtained from Sigma.

Preparation of Proteins. Activated tagless ERK2 was generated essentially as described.[23] Expression and purification of Ets-1 (1−138) was followed by the method described in the previously published literature.[30]

Peptide Synthesis and Purification. The synthesis and purification of peptides Lig-F (Ac-YAPRAPAKLAFQFPSR-NH_2) and Lig-D (FQRKTLQRRNLKGLNLNL-NH_2) have previously been reported.[18] Sub-D (Ac-QRKTLQRRNLKGLNLNL-XXX-TGPLSPGPF-NH_2; X = 6-aminohexanoic acid) and Sub-F (YAEPLTPRILAKWEWPA-NH_2) were synthesized using a Liberty CEM automated microwave peptide synthesizer by utilizing an Fmoc solid-sate peptide synthesis protocol. Sub-F was cleaved using a cleavage cocktail (1 mL of thioanisole, 0.5 mL of H_2O, 0.5 mL of ethanedithiol, and 18.0 mL of trifluoroacetic acid) for 3 h. Sub-D was acetylated at the *N*-terminus and then cleaved using a cleavage cocktail (0.75 mL of thioanisole, 0.2 mL of H_2O, 0.4 mL of ethanedithiol, and 18.65 mL of trifluoroacetic acid) for 4 h. Sub-F was subjected to an elution profile of 0−10% acetonitrile 0−5 min; 10−30% 5−60 min. Likewise, Sub D was purified with a gradient of 0−20% acetonitrile 0−5 min; 20−50% 5−60 min. Purified peptides were characterized for purity and mass by analytical HPLC (System Gold, Beckman Coulter) followed by mass spectrometry using either a MALDI-TOF (Voyager, PerSeptive Biosystem) or an ESI (LCQ, Thermo Finnigan). The following analytical results were obtained; Sub-F, obsd 2041.00, calcd mass 2040.08; Sub-D, obsd mass 3445.02, calcd mass 3446.85).

Kinase Analysis. ERK2 activity was determined as described previously.[30]

Data Analysis. *Steady-State Kinetic Experiments.* Reactions were carried out at 27 °C in kinase assay buffer (25 mM HEPES pH 7.4, 100 mM KCl, 2 mM DTT, 40 μg/mL BSA, and 20 mM $MgCl_2$) containing 2 nM ERK2 and varied concentrations of peptide substrates, Ets-1, and inhibitors. Rates were measured under conditions where total product formation represented less than 10% of the initial substrate concentrations. The reaction was incubated for 10 min before initiation by addition of enzyme and quantified as described previously.[29] Initial rates were determined by linear least-squares fitting to plots of product against time. Reciprocal plots of $1/v$ against $1/s$ were checked for linearity, before the data were fitted to eq 1 using a nonlinear least-squares approach, assuming equal variance for velocities, using the program Kaleidagraph 3.5 (Synergy software). The intercepts $1/V_{max}^{app}$ and slopes $K_{ms}^{app}/V_{max}^{app}$ obtained from these fits were then plotted against either the inhibitor concentration (i) (for inhibition experiments) or the reciprocal of the nonvaried substrate concentration ($1/s$) (for initial velocity experiments). These plots were used to determine the appearance of the overall kinetic equation. To obtain kinetic parameter K_m^{ATP} of Ets-1 phosphorylation (Table 1), a double-reciprocal plot of $1/v$ vs $1/[MgATP^{2-}]$ was obtained at 15 μM Ets-1. Values for kinetic constants were then obtained using the program Scientist (Micromath) by fitting the kinetic data to the relevant overall equation. Data conforming to a sequential initial velocity pattern were fitted to eq 2; data conforming to linear competitive inhibition were fitted to eq 3; data conforming to noncompetitive inhibition were fitted to eq 4. Dose−response curves for data conformed to hyperbolic inhibition to eq 5 and for data conformed to activation to eq 6.

Table 1. Kinetic Parameters for the Phosphorylation of Substrates by ERK2

substrate	$K_i^{peptide}$, μM	$K_m^{peptide}$, μM	K_m^{ATP}, μM	k_{cat}, s^{-1}
Sub-D	2.4 ± 1.0	2.5 ± 1.5	62 ± 42	15 ± 0.7
Sub-F	3.3 ± 1.1	5.4 ± 3.2	130 ± 110	6.5 ± 0.4
Ets	2.6 ± 1.8	2.9 ± 2.7	130 ± 100	17 ± 1

$$\frac{k_{obs}}{k_{cat}^{app}} = \frac{S}{K_{mS}^{app} + S} \quad (1)$$

$$\frac{k_{obs}}{k_{cat}} = \frac{ab}{K_{iA}K_{mB} + K_{mA}b + K_{mB}a + ab} \quad (2)$$

$$\frac{k_{obs}}{k_{cat}^{app}} = \frac{S}{K_{mS}^{app}(1 + i/K_{ic}^{app}) + S} \quad (3)$$

$$\frac{1}{k_{obs}} = \frac{K_m}{k_{cat}}\left(1 + \frac{[I]}{K_i}\right)\frac{1}{[S]} + \frac{1}{k_{cat}}\left(1 + \frac{[I]}{K_i}\right) \quad (4)$$

$$k_{obs} = \frac{k_0}{1 + (i/K_{50})} + k' \quad (5)$$

$$k_{obs} = k' - \frac{k_0}{1 + (x/K_{50})} \quad (6)$$

The parameters used in deriving equations are defined as follows: k_{obs}, observed rate constant; k_{cat}^{app}, apparent catalytic constant; s, concentration of substrate S; k_{mS}^{app}, apparent Michaelis constant for substrate S; a, concentration of substrate A; b, concentration of substrate B; K_{iA}, inhibition constant for

Scheme 1. Schematic Representation of ERK2 and the ERK2·Sub-D and ERK2·Lig-D Complexes Depicting the DRS, the FRS, and the Active Site[a]

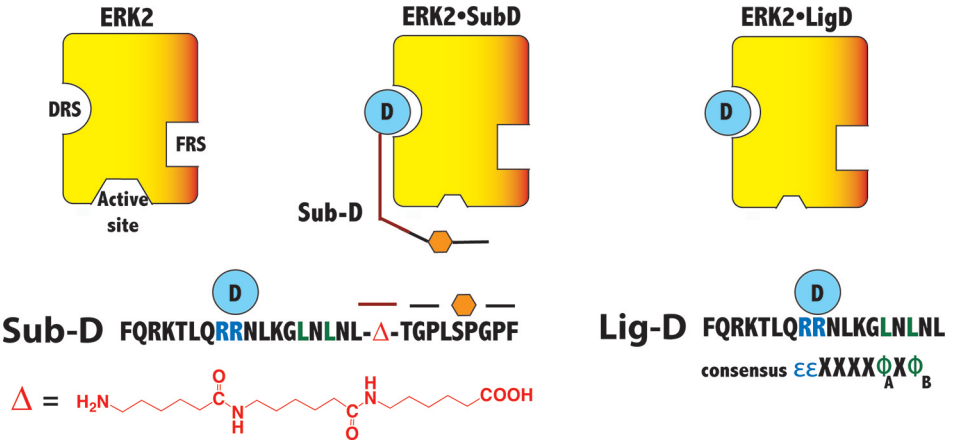

[a]The RRNLKGLNL modular docking site and consensus phosphorylation site are shown in Sub-D and Lig-D.

Scheme 2. Schematic Representation of ERK2 and the ERK2·Sub-F and ERK2·Lig-F Complexes Depicting the DRS, the FRS, and the Active Site[a]

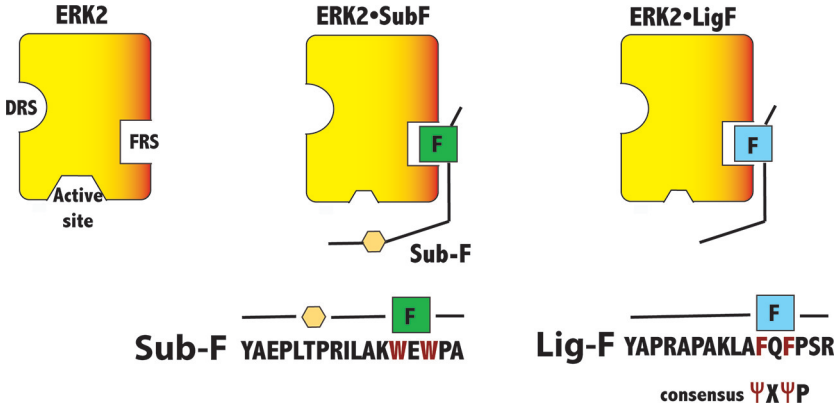

[a]The WEWP modular docking site and consensus phosphorylation site is shown in Sub-F. The Modular FQFP docking site is shown in Lig-F.

substrate A; K_{mA}, Michaelis constant for substrate A; K_{mB}, Michaelis constant for substrate B; i, concentration of inhibitor I; K_i^{app} or K_{ic}^{app}, apparent competitive inhibition constant for inhibitor I; k_0, is the observed rate constant in the absence of inhibitor; k' is the observed rate constant at saturating inhibitor, I, or activator x; K_{50} is the concentration that leads to half the maximal change in k_{obs}.

Molecular Modeling. To facilitate the virtual docking of peptides to ERK2, we constructed the initial peptide structures using Modeller9v4,[31] as described previously for Lig-D and Lig-F.[18] Here we briefly describe the approach used to model the structures of Sub-D and Sub-F onto the surface of activated ERK2: a) *FQRKTLQRRNLKGLNLNL-XXX-TGPLSPGPF* (Sub-D) - *FQRKTLQ-**RRNLKGLNLNL*** (Lig-D) was modeled as described previously.[18] Then the LEaP module in Amber 9.0[32] was used to generate a random 3-D structure of TGPLSPGPF. This was then connected to the C-terminus of Lig-D with a flexible linker to generate Sub-D. (b) *YAEPLTPRILAK**WEWP**A* (Sub-F) coordinates were first obtained for an FSFG motif as described previously for Lig-F.[18] The FSFG was then transformed to WEWP using the LEaP module[32] of Amber. Binding within the DRS, the FRS, and the active site were performed to the active form of ERK2 (PDB-ID: 2ERK)[33] as described previously with GOLD 4.1 (Cambridge Crystallographic Data Centre[18,34,35]).

RESULTS

Design of Peptide Substrates. Recently, several peptide substrates for ERK2 were described whose principle design feature was to take advantage of the modular docking strategy employed by ERK2.[11,26] Basing our design on these peptides, we developed two new substrates for ERK2 called Sub-D and Sub-F, which were expected to exhibit specific interactions with the DRS and the FRS respectively [11,26] (see Figure 1 and Schemes 1 and 2). Sub-D is comprised of a short docking sequence based on the docking site of the yeast MKK STE7, which is separated by a flexible hydrophobic linker from a C-terminal MAPK phosphorylation consensus sequence (Scheme 1). Sub-F contains a C-terminal WXWP motif (rather than the conventional FXFP motif) separated by five amino acids from a MAPK phosphorylation consensus sequence (Scheme 2). These simple modular peptide substrates offer a unique opportunity to examine features of the MAPK catalytic mechanism that are difficult to investigate using protein substrates. In particular, they allow experiments to be designed that focus on each specific docking interaction.

dx.doi.org/10.1021/bi201103b | *Biochemistry* 2011, 50, 9500–9510

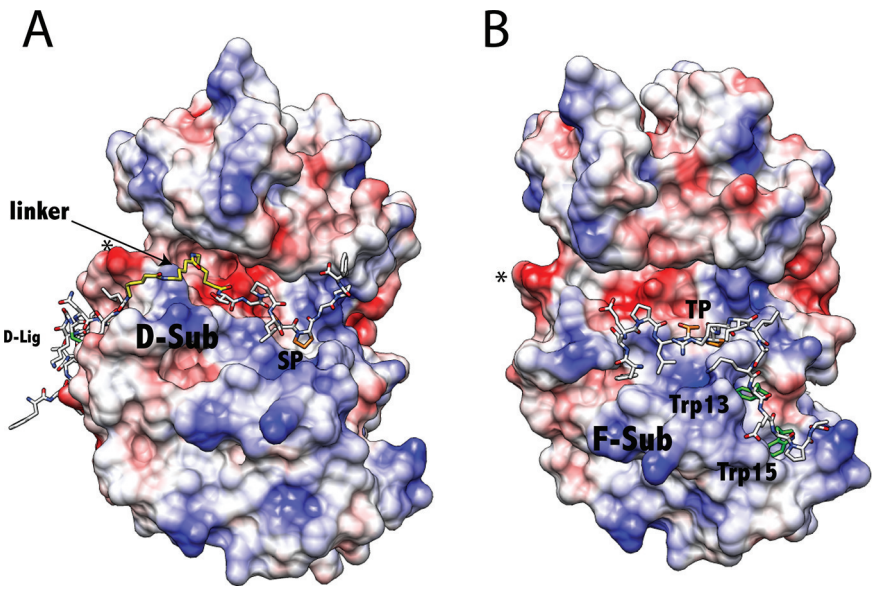

Figure 2. Molecular models of peptides bound to ERK2. (A) Sub-D (QRKTLQRRNLKGLNLNL-XXX-TGPLSPGPF) (X = 6-aminohexanoic acid) bound to the DRS of ERK2. The flexible X_3 linker (yellow) (X = 6-aminohexanoic acid) joins the Lig-D[18] moiety to the phosphorylation motif (Ser-Pro indicated). (B) Sub-F (YAEPLTPRKLAKWEWPA) bound to the FRS. The ψ–X–ψ motif of Sub-F binds the FRS. The phosphorylation motif, Thr-Pro, is indicated. Coulombic surface representation was performed in Chimera using default parameters.

2. Modeling the Binding of Modular Peptide Substrates to ERK2. Recently, using a series of biophysical approaches we determined that activated ERK2 is monomeric.[23] Therefore, potential allosteric effects due to subunit interactions within an ERK2 dimer may be discounted. Accordingly, Sub-D and Sub-F were modeled onto the surface of monomeric ERK2 using a molecular docking approach using the software GOLD 4.1 (Cambridge Crystallographic Data Centre[34,35]) (Figure 2). The docking site of Sub-D was modeled using distance restraints in a manner similar to that for the modeling of the peptide Lig-D.[18] In addition, the Thr-Pro motif was restrained within the active site as described previously for Ets-1.[21] The modeling of Sub-D to the surface of ERK2 reveals a plausible mode of binding where the D-site engages the DRS (Figure 2A). The modeling also reveals a potential pathway for the hydrophobic linker along the surface of ERK2. The top-ranked 15 structures all revealed a similar pathway. The engagement of Sub-D at the DRS is in agreement with a recent NMR study, which examined the binding of Sub-D to inactive ERK2.[14]

As noted above, a distinct hydrophobic binding pocket for the F-site, formed by the P+1 site, the αF helix, and the MAP kinase insert was first identified using hydrogen-exchange mass spectrometry [6,11] (Figure 1). This was set as the search region for the WXWP binding motif of Sub-F. After the Thr-Pro motif at the active site was restrained, our modeling studies suggest that the WXWP motif of Sub-F binds the FRS of ERK2 in a similar manner to the FXFP motif of the peptide Lig-F with the five residues that link the two motifs adopting an extended configuration (Figure 2B). These modeling studies provide the basis for understanding how ERK2 recognizes the modular peptide substrates Sub-D and Sub-F. While the predicted binding mode of the substrates may not represent the lowest energy mode of binding for each substrate, we believe that it does approach a structure the peptides must adopt in order to be phosphorylated. These models establish important features of the ERK2-peptide interactions and provide a platform from which to examine how docking interactions may affect substrate binding and catalysis of ERK2.

Kinetic Mechanisms of Modular Peptide Phosphorylation. The kinetic mechanism of peptide phosphorylation by ERK2 has not previously been reported. Therefore, in order to assess potential allostery in the catalytic mechanism we sought to first establish the mechanism. To understand the mechanism of Sub-D phosphorylation, the dependence of product formation on the concentrations of each substrate was determined by the method of initial rates using a radioactive kinase assay.[29] In each case the appearance of product with time was linear and highly reproducible to within 10%. Double-reciprocal plots of $1/v$ versus $1/[\text{Sub-D}]$ (Figure 3A) or $1/v$ versus $1/[\text{MgATP}^{2-}]$ (Figure 3B) are linear and displayed a pattern of intersecting lines on the abscissa at a common vertical coordinate. This pattern is consistent with a sequential mechanism where both substrates react before either product dissociates from the enzyme.[36] The mechanism of Sub-F phosphorylation was analyzed in a similar manner. The double-reciprocal plots of $1/v$ versus $1/[\text{Sub-F}]$ or $1/v$ versus $1/[\text{MgATP}^{2-}]$ at varied fixed concentrations of second substrate are linear and also display a pattern of intersecting lines (Figure 4A,B) consistent with a sequential mechanism where both Sub-F and MgATP react before either product dissociates from the enzyme.[36] Kinetic parameters describing a sequential mechanism were obtained by fitting the initial rate data to eq 2 (Table 1). In both cases, the kinetic parameters (e.g., K_m and K_i) indicate that there is little thermodynamic linkage between peptide substrate and ATP when bound to ERK2 (see ref 37 for a discussion of thermodynamic linkage).

A sequential mechanism can be described further as random or ordered.[36] To assess the mechanism of Sub-D and Sub-F in more detail, inhibition studies were performed and a mode of inhibition was assigned. Inhibitors are classified according to whether they affect the apparent specificity constant, k_{cat}^{app}/K_m^{app} (competitive inhibition), the apparent catalytic constant k_{cat}^{app} (uncompetitive), or both (mixed). By plotting the data in reciprocal form as $1/k_{obs}$ against $1/[\text{substrate}]$ at varied

dx.doi.org/10.1021/bi201103b | Biochemistry 2011, 50, 9500–9510

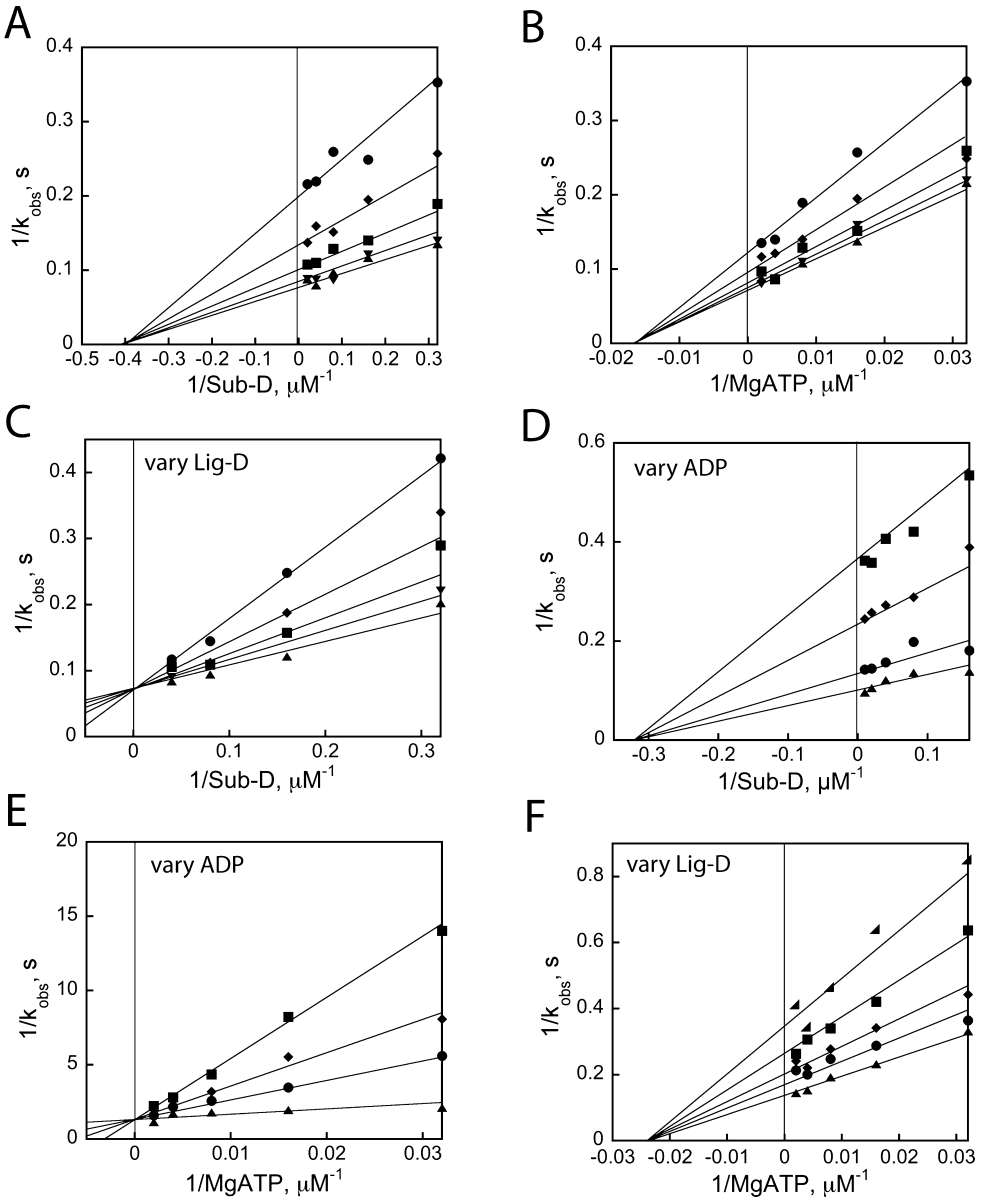

Figure 3. Substrate dependence and inhibition studies of Sub-D phosphorylation. (A) Double-reciprocal plot of $1/k_{obs}$ vs 1/[Sub-D] (3.13−50 μM) at varied fixed concentrations of MgATP (3.13−500 μM). The data were fitted to eq 2 according to k_{cat} = 15.0 ± 1.0 s^{-1}, $K_m^{Sub\text{-}D}$ = 3.0 ± 1.0 μM, K_m^{MgATP} = 62 ± 42 μM and α = 0.95 ± 0.74 s^{-1}. (B) Double reciprocal plot of $1/k_{obs}$ vs 1/MgATP (31.3−500 μM) at varied fixed concentrations of Sub-D (3.13−50 μM). The data were fitted to eq 2 according to k_{cat} = 15.0 ± 1.0 s^{-1}, $K_m^{Sub\text{-}D}$ = 3.0 ± 1.0 μM, K_m^{MgATP}= 62 ± 42 μM and α = 0.95 ± 0.74 s^{-1}. (C) Double reciprocal plot of $1/k_{obs}$ vs 1/[Sub-D] (6.25−100 μM) at varied fixed concentrations of Lig-D (0 − 40 μM) and 1 mM MgATP. Initial velocities were measured using various concentration of Sub-D (3−50 μM). The data were fitted to a model of competitive inhibition according to eq 3, where $K_m^{Sub\text{-}D}$ = 4.9 ± 0.7 μM, and k_{cat}^{app} = 10.9 ± 0.5 s^{-1}. (D) Double-reciprocal plot of $1/k_{obs}$ vs 1/[Sub-D] (6.25−100 μM) at varied fixed concentrations of MgADP (0−2000 μM) and 1 mM MgATP. The data were fitted to a model of noncompetitive inhibition according to eq 4 where $K_m^{Sub\text{-}D}$ = 3 ± 0.5 μM and k_{cat}^{app} = 10.0 ± 0.5 s^{-1}. (E) Double-reciprocal plot of $1/k_{obs}$ vs 1/[MgATP] (31.3−500 μM) at varied fixed concentrations of MgADP (0−1000 μM) and 20 μM Sub-D. The data were fitted to a model of competitive inhibition according to eq 3 where K_m^{ATP} = 27 ± 8 μM and k_{cat}^{app} = 10.0 ± 0.5 s^{-1}. (F) Double-reciprocal plot of $1/k_{obs}$ vs 1/[MgATP] at varied fixed concentrations of Lig-D (0 − 164 μM) and 20 μM Sub-D. The data were fitted to a model of noncompetitive inhibition according to eq 4 where K_m^{ATP} = 40 ± 4 μM and k_{cat}^{app} = 10.0 ± 0.5 s^{-1}.

concentrations of inhibitor one can determine the mechanism by noting whether an inhibitor affects the slope or intercept of a plot. A mode of inhibition was determined for each inhibitor/substrate pair (Tables 2 and 3).[36] The peptide Lig-D showed a competitive inhibition pattern toward Sub-D (Figure 3C) and a noncompetitive inhibition pattern toward $MgATP^{2-}$ (Figure 3F). When MgADP was used as the product inhibitor, double-reciprocal plots of $1/v$ vs 1/[S] showed a noncompetitive inhibition pattern toward Sub-D and competitive pattern for toward $MgATP^{2-}$ (Figure 3D,E). The data were fitted using eqs 2−4 (Table 2). Sub-F also follows a similar inhibition pattern to Sub-D. Lig-F showed a competitive inhibition pattern toward Sub-F (Figure 4C) and a noncompetitive inhibition pattern toward $MgATP^{2-}$ (Figure 4F). When MgADP was used as the inhibitor, double-reciprocal plots of $1/v$ versus 1/[S] showed a noncompetitive inhibition pattern

dx.doi.org/10.1021/bi201103b | Biochemistry 2011, 50, 9500−9510

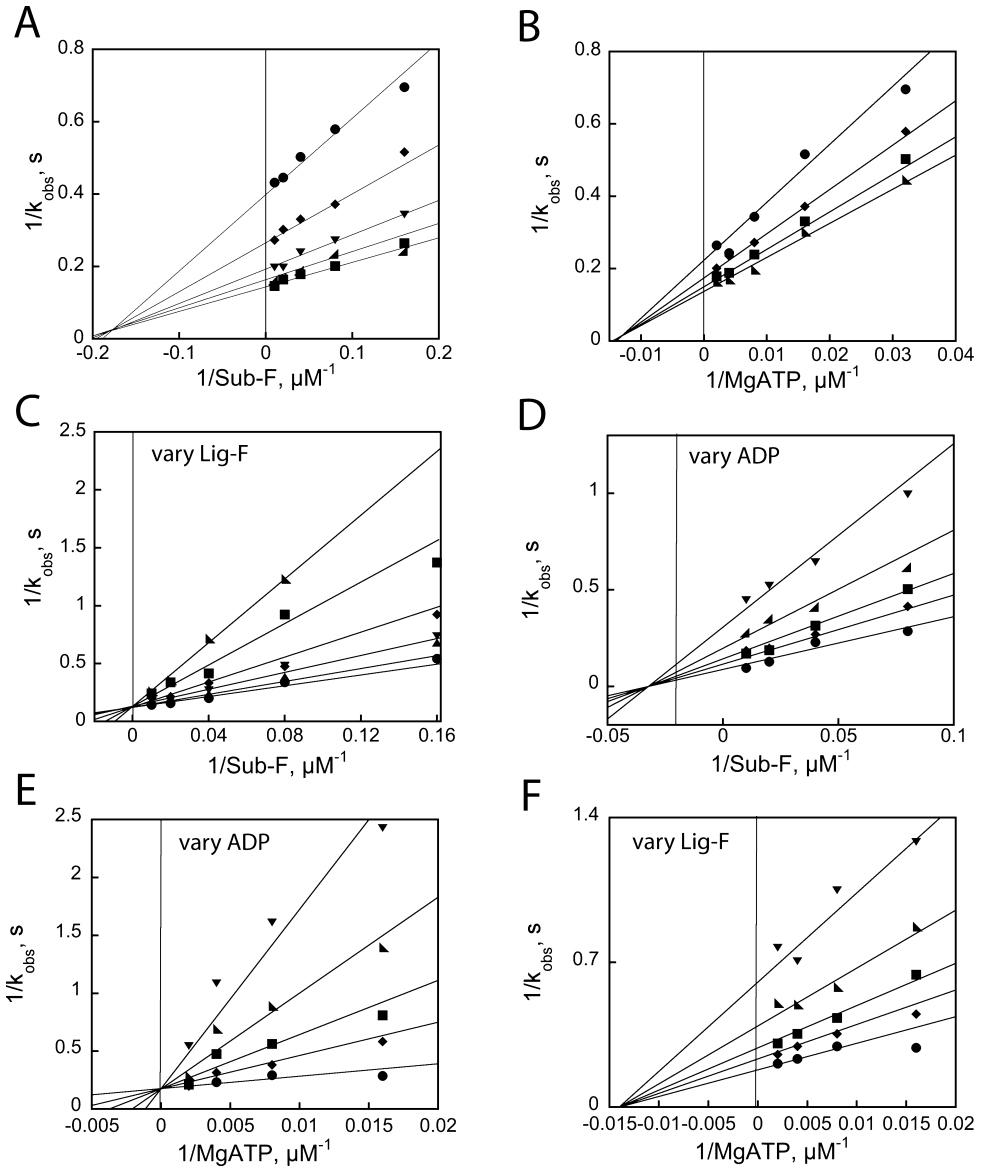

Figure 4. Substrate dependence and inhibition of the phosphorylation of Sub-F. (A) Double-reciprocal plot of $1/k_{obs}$ vs 1/Sub-F (6.25−100 μM) at varied fixed concentrations of MgATP (31.3−500 μM). The lines correspond to the best fit to eq 2 according to $k_{cat} = 6.5 \pm 0.4\ s^{-1}$, $K_m^{Sub\text{-}F} = 5.4 \pm 3.2\ \mu M$, $K_m^{MgATP} = 130 \pm 100\ \mu M$, and $\alpha = 0.98 \pm 0.74\ s^{-1}$. (B) Double-reciprocal plot of $1/k_{obs}$ vs 1/MgATP (31.3−500 μM) at varied fixed concentrations of Sub-F (6.25−100 μM). The lines correspond to the best fit to eq 2 according to $k_{cat} = 6.5 \pm 0.4\ s^{-1}$, $K_m^{Sub\text{-}F} = 5.4 \pm 3.2\ \mu M$, $K_m^{MgATP} = 130 \pm 100\ \mu M$, and $\alpha = 0.98 \pm 0.74\ s^{-1}$. (C) Double-reciprocal plot of $1/k_{obs}$ vs 1/[Sub-F] (6.25−100 μM) at varied fixed concentrations of Lig-F (0−168 μM) and 1 mM MgATP. The data were fitted to a model of competitive inhibition according to eq 3, where $K_m^{Sub\text{-}F} = 5.4 \pm 0.7\ \mu M$, $k_{cat}^{app} = 7.6 \pm 0.4\ s^{-1}$, and $K_{ic}^{Lig\text{-}F} = 26 \pm 5\ \mu M$. (D) Double-reciprocal plot of $1/k_{obs}$ vs 1/Sub-F (6.25−100 μM) and varied fixed concentrations of MgADP (0−2000 μM) and 1 mM MgATP. The data were fitted to a model of noncompetitive inhibition according to eq 4 where $K_m^{Sub\text{-}F} = 6.3 \pm 2.4\ \mu M$ and $k_{cat}^{app} = 5.5 \pm 0.5\ s^{-1}$. (E) Double reciprocal plot of $1/k_{obs}$ vs 1/[MgATP] (31.25−500 μM) at varied fixed concentrations of MgADP (0−1000 μM) and 15 μM Sub-F. The data were fitted to a model of competitive inhibition according to eq 3 where $K_m^{ATP} = 41 \pm 10\ \mu M$ and $k_{cat}^{app} = 5.5 \pm 0.5\ s^{-1}$. (F) Double-reciprocal plot of $1/k_{obs}$ vs 1/[MgATP] at varied fixed concentrations of Lig-F (0−164 μM) and 15 μM Sub-F. The data were fitted to a model of noncompetitive inhibition according to the eq 4 where $K_m^{ATP} = 71 \pm 10\ \mu M$ and $k_{cat}^{app} = 5.8 \pm 0.5\ s^{-1}$.

toward Sub-F and a competitive pattern for toward $MgATP^{2-}$ (Figure 4D,E). The data were fitted using eqs 2−4 (Table 3).

ERK2 is known to phosphorylate the protein substrate Ets-1 through a random-order mechanism,[29] and the plots shown in Figures 3 and 4 are consistent with a similar random-order mechanism for the phosphorylation of the peptide substrates. A steady-state ordered mechanism can be excluded; it predicts an uncompetitive pattern of inhibition for one of the substrate−inhibitor pairs. It should be noted that ADP may be regarded as a dead-end inhibitor. Although it is a product of the reaction it is unlikely to effect a significant reversal of any of the forward steps of the reaction because the formation of products on the enzyme is expected to be highly favorable.[21] Furthermore, ADP is expected to bind ERK2 to form an abortive ternary complex in the presence of either of the peptide substrates.[29]

Specificity of ERK2 When Complexed to an Exogenous Docking Site Mimic. The kinetic data establishes that both peptides are phosphorylated with a catalytic efficiency that compares to the bona fide protein substrate Ets-1.[38] Together with the modeling these data suggest that both peptides

dx.doi.org/10.1021/bi201103b | Biochemistry 2011, 50, 9500−9510

Table 2. Inhibition Patterns for the Phosphorylation of Sub-D by ERK2

varied substrate	fixed substrate	inhibitor	mechanism	K_i^{app} (μM)
Sub-D	MgATP	Lig-D	competitive	20 ± 4[a]
MgATP	Sub-D	Lig-D	noncompetitive	108 ± 8[b]
Sub-D	MgATP	MgADP	noncompetitive	730 ± 56[b]
MgATP	Sub-D	MgADP	competitive	91 ± 25[a]

[a]The parameters are the best fits according to eq 3 for competitive inhibition. [b]The parameters are the best fits according to eq 4 for noncompetitive inhibition (Figure 3).

Table 3. Inhibition Patterns for the Phosphorylation of Sub-F by ERK2

varied substrate	fixed substrate	inhibitor	mechanism	K_i^{app} (μM)
Sub-F	MgATP	Lig-F	competitive	26 ± 5[a]
MgATP	Sub-F	Lig-F	noncompetitive	81 ± 10[b]
Sub-F	MgATP	MgADP	noncompetitive	808 ± 78[b]
MgATP	Sub-F	MgADP	competitive	132 ± 28[a]

[a]The parameters are the best fits according to eq 3 for competitive inhibition. [b]The parameters are the best fits according to eq 4 for noncompetitive inhibition (Figure 4).

represent excellent monodocking substrates with which to examine the importance of each recruitment site within the context of ERK2 catalysis. Two important questions can now be addressed using these peptides: (1) does a peptide that binds the FRS block the ability of ERK2 to phosphorylate Sub-D and (2) is there evidence of allosteric communication from the recruiting sites to distal sites on ERK2. To address both questions, we examined the ability of ERK2 to phosphorylate either peptide in the absence or presence of saturating peptide ligands (Lig-D and Lig-F; see Schemes 1 and 2) that target the DRS and the FRS, respectively.[18] Modeling (not shown) suggested that Lig-D does not compete in a steric manner with Sub-F for binding to ERK2. Similarly, Lig-F is not predicted to compete in a steric manner with Sub-D. Thus, any effects of Lig-D on Sub-F phosphorylation or Lig-F on Sub-D phosphorylation may be interpreted as allosteric in origin.

First we assessed whether docking at the FRS blocks the ability of ERK2 to phosphorylate Sub-D. The phosphorylation of Sub-D (at its K_m of ~3 μM) was determined in the presence of 1 mM MgATP and an increasing concentration of Lig-F. Notably, Lig-F has no effect on k_{obs} for the phosphorylation of Sub-D under these experimental conditions (Figure 5A, ■). In a control experiment Lig-F was shown to exhibit a dose-dependent decrease in the phosphorylation of Sub-F (Figure 5B, ■). To our knowledge this demonstrates for the first time that an F-site ligand is not a universal ERK2 inhibitor. Furthermore, these data are consistent with the notion that canonical docking interactions at the FRS are not strongly coupled to the active site or the DRS of activated ERK2.

When the phosphorylation of Sub-F (at its K_m of 15 μM) was determined in the presence of 1 mM MgATP and an increasing concentration of Lig-D a very slight dose-dependent increase in k_{obs} was observed as the concentration of Lig-D was increased (Figure 5B, ○). Conversely, the peptide decreased the ability of ERK2 to phosphorylate Sub-D in a dose-dependent manner (Figure 5A, ○). A full kinetic analysis in the presence of saturating Lig-D (Figure 5C) suggests that the binding of Lig-D to ERK2 induces a 1.3 ± 0.1-fold increase in k_{cat} without affecting the binding of ATP or the peptide. These experiments suggest that docking interactions at the DRS are weakly coupled to the active site but uncoupled to the FRS and further show that the DRS can be occupied without hindering the catalytic ability of ERK2.

■ DISCUSSION

Docking interactions at the DRS or the FRS (Figure 1) represent a key mechanism to affect cellular signaling involving ERK2, as they mediate the specificity and the efficiency of all the catalytic processes involving downstream substrates.[39] Therefore, they have attracted considerable interest as possible targets for the development of non-ATP competitive inhibitors (reviewed in ref 4). Efforts to understand the role of docking interactions in mediating substrate recognition and turnover have been hampered by the lack of crystal structures of

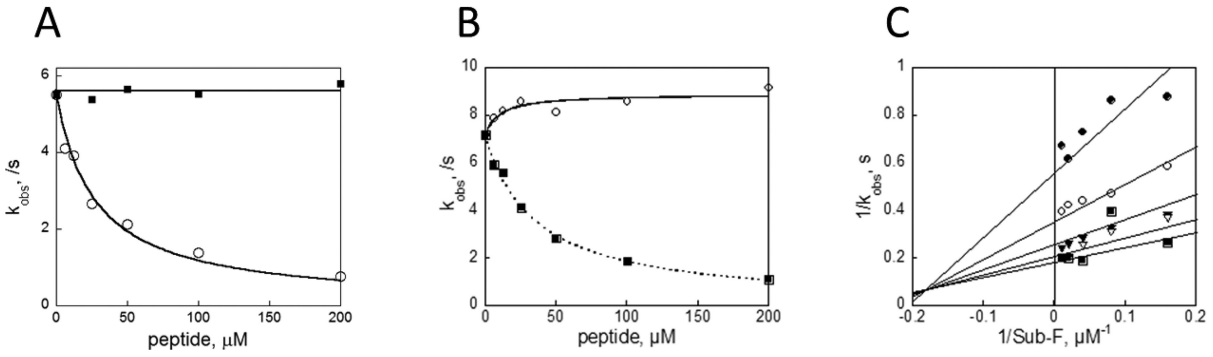

Figure 5. Sensitivity of ERK2 to docking site occupancy. (A) Dose−response curve for the effect of Lig-F (■) or Lig-D (○) on the ability of ERK2 to phosphorylate Sub-D (3 μM) in the presence of 1 mM MgATP. The line through the closed squares (Lig-F) corresponds to a linear fit. The line through the open circles (Lig-D) corresponds to the best fit to eq 5 for a dose−response curve for competitive inhibition, where k_0 = 5.3 ± 0.2 s^{-1} and k_{50} = 30 ± 4 μM. (B) Dose−response curve for the effect of Lig-F (■) or Lig-D (○) on the ability of ERK2 to phosphorylate Sub-F (15 μM) in the presence of 1 mM MgATP. The line through the closed squares (Lig-F) corresponds to the best fit to eq 5 for a dose−response curve for a competitive inhibitor where k_0 = 7.2 ± 0.1 s^{-1} and K_{50} = 35 ± 3 μM. The line through the open circles (Lig-D) corresponds to the best fit to eq 6 for a dose−response curve to an activator where k_0 = 7.2 ± 0.3 s^{-1}, k' = 8.9 ± 0.3 s^{-1}, and K_{50} = 10 ± 8 μM. (C) Double-reciprocal plot of $1/k_{obs}$ vs 1/Sub-F at various concentrations of MgATP (31−500 μM) with a saturating concentration of Lig-D (100 μM). The lines correspond to the best fit to eq 2 where k_{cat} = 8.0 ± 0.3 s^{-1}, $K_i^{Sub\text{-}F}$ = 5 ± 2 μM, $K_m^{Sub\text{-}F}$ = 5.6 ± 2.1 μM, and K_m^{MgATP} = 76 ± 33 μM.

dx.doi.org/10.1021/bi201103b | Biochemistry 2011, 50, 9500−9510

ERK2·substrate complexes. However, a recent experimentally and computationally derived model for the complex between ERK2 and the transcription factor Ets-1 has revealed, for the first time, how two docking interactions can position a phosphorylation site within proximity of the active site.[18] This study shows how the disordered *N*-terminus of Ets-1 docks to the DRS and stabilizes the ERK·Ets-1 complex by approximately 10-fold.[18] In addition, the study also suggests that Ets-1 binds the MAPK insert of ERK2 through its SAM domain.[18]

While three crystal structures are available to illustrate docking interactions at the DRS of unactivated ERK2,[12,40,41] no crystallographic information is currently available to reveal interactions at the FRS. However, HXMS data coupled to site-directed mutagenesis and computational modeling has been invaluable in providing some insight into the nature of docking at the FRS.[6] These data have enabled mutagenesis experiments to be designed to impair docking interactions, which have identified substrates that utilize just the DRS, the FRS, or both.[19]

In the present study, we designed two new peptide substrates, Sub-D and Sub-F, to investigate whether allosteric effects at ERK2 recruitment sites underlie catalysis and/or inhibition of ERK2 (Schemes 1 and 2). In particular, we were interested in learning the underlying mechanism by which peptides containing F-sites inhibit the activity of ERK2 toward protein substrates.

The modeling studies (Figure 2) suggest how docking interactions facilitate the binding of both peptides to ERK2. For example, a key feature of the ERK2·Sub-D model (Figure 2A) is that the docking interaction of the RRXXXXLXL sequence of Sub-D at the Φ_{chg} site of the DRS position the linker to thread loosely along the groove of the DRS, somewhat reminiscent of the manner in which the intrinsically disordered *N*-terminus of Ets-1 may engage the same groove.[18] Presumably, the docking as well as the weak association of the linker promotes interaction of the consensus phosphorylation site, PLSP, with the active site. Sub-F contains a WXW motif, previously shown to facilitate recognition by ERK2.[11] The docking interactions of the WXW motif of Sub-F at the FRS, appears to provide sufficient auxiliary interactions to promote the weak association of Sub-F to the surface of ERK2. Again, these docking interactions allow the appropriate binding of the consensus phosphorylation sequence.

The mechanistic studies (Figures 3 and 4) are consistent with both Sub-D and Sub-F being phosphorylated through a random-order sequential mechanism. Both peptides are efficiently phosphorylated by ERK2 with k_{cat}/K_m values of 6×10^6 M^{-1} s^{-1} and 2×10^6 M^{-1} s^{-1} for Sub-D[a] and Sub-F, respectively. Both peptides are phosphorylated with efficiency similar to that of the protein substrate Ets-1 (6×10^6 M^{-1} s^{-1}).[29] Thus, peptide substrates that exclusively target either the DRS or the FRS may be phosphorylated with equal efficiency to a bona fide protein substrate. Unlike peptides that were tested previously as substrates,[11] Sub-F does not exhibit pronounced substrate inhibition and in this respect represents a useful ERK2 substrate for the evaluation of FRS-directed non-ATP competitive inhibitors.

The kinetic parameters for both Sub-D and Sub-F suggest that the binding affinity of neither peptide is substantially affected by the binding of MgATP to the active site. An absence of thermodynamic linkage[37] between the peptides and ATP is consistent with there being little coupling between the ATP binding site and either of the two recruitment sites in activated ERK2.

Modeling suggests that Lig-F inhibits the phosphorylation of Ets-1 through a steric mechanism as the binding of Lig-F to the FRS appears to block the binding of the SAM domain to the MAPK insert. Based on a similar analysis, we reasoned that the phosphorylation of Sub-D will not be subject to steric inhibition by Lig-F. Therefore, we tested whether Lig-F inhibits Sub-D phosphorylation to provide evidence for a possible allosteric mechanism. Significantly, Lig-F has no effect on the ability of ERK2 to phosphorylate Sub-D (Figure 5A). In contrast, Lig-F competitively inhibits Sub-F. These data demonstrate, for the first time, that peptides bound to the FRS probably inhibit protein substrate phosphorylation through a steric mechanism. The data also provide support for the notion that small molecule inhibitors that bind the FRS may be developed to exhibit substrate-selective inhibition. The ability to inhibit the activation of a specific subset of ERK2 substrates may provide unique opportunities in the development of therapeutics. In this respect it is interesting that F-site-mediated phosphorylation of IEG-products, such as c-fos and c-Myc leads to the prolongation of their nuclear expression and activity by several hours.[42−45] The selective inhibition of these immediate early genes might provide significant therapeutic benefit.

The studies also show that a peptide ligand bound to the DRS does not inhibit the phosphorylation of a substrate utilizing the FRS. In fact, the slight 1.3 ± 0.1-fold increase in k_{cat} observed for the phosphorylation of Sub-F suggests there can be favorable, but weak coupling between the DRS and the active site in activated ERK2. A number of studies support the notion that MAPKs may stably associate with some substrates following cell stimulation. For example, ERK2 is reported to stably associate with RSK3[46] and the nuclear pore protein Tpr,[47] following cell stimulation and studies in yeast suggest that MAPKs become physically associated with genes through association with various proteins, including transcription factors, following cell stimulation.[48−52] The kinetic studies reported here demonstrate that docking sites that interact with either the DRS, or the FRS have little effect on the intrinsic catalytic activity of ERK2. Furthermore, they suggest that ERK2 complexes mediated by the DRS may be capable of phosphorylating substrates that utilize the FRS. Recently, we showed that activated ERK2 is monomeric.[23] Thus, the ERK2·RSK3 complex, which is thought to be mediated by docking to the DRS [5] is predicted on the basis of this study to exhibit an exclusive activity toward substrates containing F-sites. In contrast the ERK·Tpr complex, which is mediated by the FRS, is likely to be catalytically inactive due to steric effects.

■ CONCLUSION

Single docking interactions at either the DRS or the FRS promote efficient phosphorylation of a peptide substrate with a specificity constant comparable to a bona fide protein substrate. On the basis of the use of peptide probes there appears to be limited allosteric communication within the ERK2 monomer between the active site, the FRS, and the DRS. Docking interactions on activated ERK2 may be characterized as both spatially discrete as well as functionally independent. Activated ERK2 that is directly recruited to cellular locations through binding to its DRS may selectively phosphorylate substrates containing F-sites. Such recruitment may serve as an additional tier of ERK2 regulation. Peptide sequences that target the FRS

are likely to block ERK2 activity through a steric mechanism. However, smaller molecules may be designed to target the FRS and exhibit selectivity for substrates that utilize the FRS exclusively.

AUTHOR INFORMATION

Corresponding Author

*Tel: 512-471-9267/512-232-1832. Fax: 512-232-2606. E-mail: (K.N.D.) kinases@me.com; (P.R.) pren@mail.utexas.edu.

Author Contributions

^These authors contributed equally.

Funding

This research was supported in part by grants from the Welch Foundation (F-1390) to K.N.D. and the National Institutes of Health to K.N.D. (GM59802) and to P.R. (GM79686).

ABBREVIATIONS

ATP, adenosine triphosphate; BSA, bovine serum albumin fraction V; DTT, dithiothreitol; EDTA, ethylene diamine tetraacetic acid; EGTA, ethylene glycerol-bis[2-aminoethyl ether]-*N*,*N*,*N*′,*N*′-tetraacetic acid; HEPES, *N*-(2-hydroxyethyl)-piperazine-*N*′-2-ethanesulfonic acid; HTS, high throughput screening; IPTG, isopropyl-*β*-D-thiogalactopyranoside; ERK, extracellular signal-regulated protein kinase; Ets, murine (His_6-tagged)Ets1(1−138); MAPK, mitogen-activated protein kinase; IEG, Immediate early gene; MK2, mitogen-activated protein kinase activated protein kinase; MKK1, MAP kinase kinase 1; PCR, polymerase chain reaction; ESI, electrospray ionization; Sub-D, FQRKTLQRRLKGLNLNL-XXX-TGPLSPGPF (*X* = 6-aminohexanoic acid); Sub-F, YAEPL*T*PRILAKWEWPA, Lig-D, FQRKTLQRRLKGLNLNL; Lig-F, YAPRAPAKLAFQFPSR

ADDITIONAL NOTE

[a]Sub-D is similar to the previously described modular peptide;[26] however, Sub-D has a longer, more hydrophobic linker, suggesting that the precise nature of the linker is not critical for efficient phosphorylation.

REFERENCES

(1) Avruch, J. (2007) MAP kinase pathways: the first twenty years. *Biochim. Biophys. Acta 1773*, 1150−1160.

(2) Raman, M., Chen, W., and Cobb, M. H. (2007) Differential regulation and properties of MAPKs. *Oncogene 26*, 3100−3112.

(3) Barsyte-Lovejoy, D., Galanis, A., and Sharrocks, A. D. (2002) Specificity determinants in MAPK signaling to transcription factors. *J. Biol. Chem. 277*, 9896−9903.

(4) Schnieders, M. J., Kaoud, T. S., Yan, C., Dalby, K. N., and Ren, P. (2011) Computational Insights for the Discovery of Non-ATP Competitive Inhibitors of MAP Kinases. *Curr. Pharm. Des.*, in press.

(5) Tanoue, T., Maeda, R., Adachi, M., and Nishida, E. (2001) Identification of a docking groove on ERK and p38 MAP kinases that regulates the specificity of docking interactions. *EMBO J. 20*, 466−479.

(6) Lee, T., Hoofnagle, A. N., Kabuyama, Y., Stroud, J., Min, X., Goldsmith, E. J., Chen, L., Resing, K. A., and Ahn, N. G. (2004) Docking motif interactions in MAP kinases revealed by hydrogen exchange mass spectrometry. *Mol. Cell 14*, 43−55.

(7) Callaway, K. A., Rainey, M. A., Riggs, A. F., Abramczyk, O., and Dalby, K. N. (2006) Properties and regulation of a transiently assembled ERK2.Ets-1 signaling complex. *Biochemistry 45*, 13719−13733.

(8) Biondi, R. M., and Nebreda, A. R. (2003) Signalling specificity of Ser/Thr protein kinases through docking-site-mediated interactions. *Biochem. J. 372*, 1−13.

(9) Galanis, A., Yang, S. H., and Sharrocks, A. D. (2001) Selective targeting of MAPKs to the ETS domain transcription factor SAP-1. *J. Biol. Chem. 276*, 965−973.

(10) Jacobs, D., Glossip, D., Xing, H., Muslin, A. J., and Kornfeld, K. (1999) Multiple docking sites on substrate proteins form a modular system that mediates recognition by ERK MAP kinase. *Genes Dev. 13*, 163−175.

(11) Sheridan, D. L., Kong, Y., Parker, S. A., Dalby, K. N., and Turk, B. E. (2008) Substrate discrimination among mitogen-activated protein kinases through distinct docking sequence motifs. *J. Biol. Chem. 283*, 19511−19520.

(12) Liu, S., Sun, J. P., Zhou, B., and Zhang, Z. Y. (2006) Structural basis of docking interactions between ERK2 and MAP kinase phosphatase 3. *Proc. Natl. Acad. Sci. U.S.A. 103*, 5326−5331.

(13) Tanoue, T., Adachi, M., Moriguchi, T., and Nishida, E. (2000) A conserved docking motif in MAP kinases common to substrates, activators and regulators. *Nat. Cell Biol. 2*, 110−116.

(14) Piserchio, A., Warthaka, M., Devkota, A. K., Kaoud, T. S., Lee, S., Abramczyk, O., Ren, P., Dalby, K. N., and Ghose, R. (2011) Solution NMR Insights into Docking Interactions Involving Inactive ERK2. *Biochemistry 50*, 3660−3672.

(15) Jacobs, D., Beitel, G. J., Clark, S. G., Horvitz, H. R., and Kornfeld, K. (1998) Gain-of-function mutations in the Caenorhabditis elegans lin-1 ETS gene identify a C-terminal regulatory domain phosphorylated by ERK MAP kinase. *Genetics 149*, 1809−1822.

(16) Jacobs, D., Glossip, D., Xing, H., Muslin, A. J., and Kornfeld, K. (1999) Multiple docking sites on substrate proteins form a modular system that mediates recognition by ERK MAP kinase. *Genes Dev. 13*, 163−175.

(17) Fantz, D. A., Jacobs, D., Glossip, D., and Kornfeld, K. (2001) Docking sites on substrate proteins direct extracellular signal-regulated kinase to phosphorylate specific residues. *J. Biol. Chem. 276*, 27256−27265.

(18) Lee, S., Warthaka, M., Yan, C., Kaoud, T. S., Piserchio, A., Ghose, R., Ren, P., and Dalby, K. N. (2011) A model of a MAPK*substrate complex in an active conformation: a computational and experimental approach. *PLoS One 6*, e18594.

(19) Burkhard, K. A., Chen, F., and Shapiro, P. (2011) Quantitative analysis of ERK2 interactions with substrate proteins: roles for kinase docking domains and activity in determining binding affinity. *J. Biol. Chem. 286*, 2477−2485.

(20) Abramczyk, O., Rainey, M. A., Barnes, R., Martin, L., and Dalby, K. N. (2007) Expanding the repertoire of an ERK2 recruitment site: cysteine footprinting identifies the D-recruitment site as a mediator of Ets-1 binding. *Biochemistry 46*, 9174−9186.

(21) Callaway, K., Waas, W. F., Rainey, M. A., Ren, P., and Dalby, K. N. (2010) Phosphorylation of the transcription factor Ets-1 by ERK2: rapid dissociation of ADP and phospho-Ets-1. *Biochemistry 49*, 3619−3630.

(22) Dimitri, C. A., Dowdle, W., MacKeigan, J. P., Blenis, J., and Murphy, L. O. (2005) Spatially separate docking sites on ERK2 regulate distinct signaling events in vivo. *Curr. Biol. 15*, 1319−1324.

(23) Kaoud, T. S., Devkota, A. K., Harris, R., Rana, M. S., Abramczyk, O., Warthaka, M., Lee, S., Girvin, M. E., Riggs, A. F., and Dalby, K. N. (2011) Activated ERK2 Is a Monomer in Vitro with or without Divalent Cations and When Complexed to the Cytoplasmic Scaffold PEA-15. *Biochemistry 50*, 4568−4578.

(24) Gonzalez, F. A., Raden, D. L., and Davis, R. J. (1991) Identification of substrate recognition determinants for human ERK1 and ERK2 protein kinases. *J. Biol. Chem. 266*, 22159−22163.

(25) Haycock, J. W. (2002) Peptide substrates for ERK1/2: structure-function studies of serine 31 in tyrosine hydroxylase. *J. Neurosci. Methods 116*, 29−34.

(26) Fernandes, N., Bailey, D. E., Vanvranken, D. L., and Allbritton, N. L. (2007) Use of docking peptides to design modular substrates with high efficiency for mitogen-activated protein kinase extracellular signal-regulated kinase. *ACS Chem. Biol. 2*, 665−673.

(27) Fernandes, N., and Allbritton, N. L. (2009) Effect of the DEF motif on phosphorylation of peptide substrates by ERK. *Biochem. Biophys. Res. Commun. 387*, 414−418.
(28) Sheridan, D. L., Kong, Y., Parker, S. A., Dalby, K. N., and Turk, B. E. (2008) Substrate discrimination among mitogen-activated protein kinases through distinct docking sequence motifs. *J. Biol. Chem. 283*, 19511−19520.
(29) Waas, W. F., and Dalby, K. N. (2002) Transient protein-protein interactions and a random-ordered kinetic mechanism for the phosphorylation of a transcription factor by extracellular-regulated protein kinase 2. *J. Biol. Chem. 277*, 12532−12540.
(30) Waas, W. F., Rainey, M. A., Szafranska, A. E., and Dalby, K. N. (2003) Two rate-limiting steps in the kinetic mechanism of the serine/threonine specific protein kinase ERK2: a case of fast phosphorylation followed by fast product release. *Biochemistry 42*, 12273−12286.
(31) Eswar, N., Webb, B., Marti-Renom, M. A., Madhusudhan, M. S., Eramian, D., Shen, M. Y., Pieper, U., Sali, A. (2006) Comparative protein structure modeling using Modeller. *Curr. Protoc. Bioinformatics* Chapter 5, Unit 5 6.
(32) Case, D. A., Cheatham, T. E. III, Darden, T., Gohlke, H., Luo, R., Merz, K. M. Jr., Onufriev, A., Simmerling, C., Wang, B., and Woods, R. J. (2005) The Amber biomolecular simulation programs. *J. Comput. Chem. 26*, 1668−1688.
(33) Canagarajah, B. J., Khokhlatchev, A., Cobb, M. H., and Goldsmith, E. J. (1997) Activation mechanism of the MAP kinase ERK2 by dual phosphorylation. *Cell 90*, 859−869.
(34) Eldridge, M. D., Murray, C. W., Auton, T. R., Paolini, G. V., and Mee, R. P. (1997) Empirical scoring functions: I. The development of a fast empirical scoring function to estimate the binding affinity of ligands in receptor complexes. *J. Comput. Aided Mol. Des. 11*, 425−445.
(35) Jones, G., Willett, P., Glen, R. C., Leach, A. R., and Taylor, R. (1997) Development and validation of a genetic algorithm for flexible docking. *J. Mol. Biol. 267*, 727−748.
(36) Segel, I. H. (1975) *Enzyme kinetics: behavior and analysis of rapid equilibrium and steady-state enzyme systems*, Wiley-Interscience, New York, London.
(37) Reinhart, G. D. (1983) The determination of thermodynamic allosteric parameters of an enzyme undergoing steady-state turnover. *Arch. Biochem. Biophys. 224*, 389−401.
(38) Waas, W. F., and Dalby, K. N. (2001) Purification of a model substrate for transcription factor phosphorylation by ERK2. *Protein Expr. Purif. 23*, 191−197.
(39) Remenyi, A., Good, M. C., and Lim, W. A. (2006) Docking interactions in protein kinase and phosphatase networks. *Curr. Opin. Struct. Biol. 16*, 676−685.
(40) Zhou, T. J., Sun, L. G., Humphreys, J., and Goldsmith, E. J. (2006) Docking interactions induce exposure of activation loop in the MAP kinase ERK2. *Structure 14*, 1011−1019.
(41) Ma, W., Shang, Y., Wei, Z., Wen, W., Wang, W., and Zhang, M. (2010) Phosphorylation of DCC by ERK2 is facilitated by direct docking of the receptor P1 domain to the kinase. *Structure 18*, 1502−1511.
(42) Kovary, K., and Bravo, R. (1992) Existence of different Fos/Jun complexes during the G0-to-G1 transition and during exponential growth in mouse fibroblasts: differential role of Fos proteins. *Mol. Cell. Biol. 12*, 5015−5023.
(43) Murphy, L. O., Smith, S., Chen, R. H., Fingar, D. C., and Blenis, J. (2002) Molecular interpretation of ERK signal duration by immediate early gene products. *Nat. Cell Biol. 4*, 556−564.
(44) Murphy, L. O., MacKeigan, J. P., and Blenis, J. (2004) A network of immediate early gene products propagates subtle differences in mitogen-activated protein kinase signal amplitude and duration. *Mol. Cell. Biol. 24*, 144−153.
(45) Murphy, L. O., and Blenis, J. (2006) MAPK signal specificity: the right place at the right time. *Trends Biochem. Sci. 31*, 268−275.
(46) Roux, P. P., Richards, S. A., and Blenis, J. (2003) Phosphorylation of p90 ribosomal S6 kinase (RSK) regulates extracellular signal-regulated kinase docking and RSK activity. *Mol. Cell. Biol. 23*, 4796−4804.
(47) Vomastek, T., Iwanicki, M. P., Burack, W. R., Tiwari, D., Kumar, D., Parsons, J. T., Weber, M. J., and Nandicoori, V. K. (2008) Extracellular signal-regulated kinase 2 (ERK2) phosphorylation sites and docking domain on the nuclear pore complex protein Tpr cooperatively regulate ERK2-Tpr interaction. *Mol. Cell. Biol. 28*, 6954−6966.
(48) Proft, M., and Struhl, K. (2002) Hog1 kinase converts the Sko1-Cyc8-Tup1 repressor complex into an activator that recruits SAGA and SWI/SNF in response to osmotic stress. *Mol. Cell 9*, 1307−1317.
(49) Alepuz, P. M., Jovanovic, A., Reiser, V., and Ammerer, G. (2001) Stress-induced map kinase Hog1 is part of transcription activation complexes. *Mol. Cell 7*, 767−777.
(50) Pokholok, D. K., Zeitlinger, J., Hannett, N. M., Reynolds, D. B., and Young, R. A. (2006) Activated signal transduction kinases frequently occupy target genes. *Science 313*, 533−536.
(51) de Nadal, E., and Posas, F. (2010) Multilayered control of gene expression by stress-activated protein kinases. *EMBO J. 29*, 4−13.
(52) Edmunds, J. W., and Mahadevan, L. C. (2004) MAP kinases as structural adaptors and enzymatic activators in transcription complexes. *J. Cell Sci. 117*, 3715−3723.